Experiences in the Use of Composite Material for a Wing Skin

Clinton V. Eckstrom*
NASA Langley Research Center, Hampton, Virginia
and
Charles V. Spain†
Kentron Technical Center, Hampton, Virginia

Experiences in using composite skin material on an aeroelastic reserach wing used in flight flutter testing are described. Significant variations in skin shear modulus due to stress and temperature were encountered with the original fiberglass laminate skin designed to minimize wing torsional stiffness. These variations, along with the sensitivity of wing torsional stiffness to the skin-to-frame attachment method, complicated the structural model virbration mode predictions. A wing skin redesign with different fiber orientation and a reduction in the amount of skin-to-frame bonding resulted in more predictable modal characteristics without sacrificing design objectives. Design and modeling considerations for future applications are discussed.

Introduction

THE NASA Drones for Aerodynamic and Structural Testing (DAST) program invovles flight testing of aeroelastic research wings (ARW) mated to remotely piloted research vehicles.[1] Firebee II (BQM-34F) target drone aircraft have been converted for this application, primarily by replacement of the standard flight control system with a proportional control system and replacement of the standard wing with the research wings. The first of the research wings (ARW-1) was purposely designed to encounter flutter well within the flight envelope, so that an active control system for flutter suppression could be investigated. In order for the wing to withstand normal flight loads, yet encounter flutter, it was necessary to make the wing strong in bending but weak in torsion. These and other design requirements necessitated the use of a composite material for the wing skin that was matrix (resin) rather than fiber dominant in resistance to shear loads. Use of the matrix-dominant skin, however, complicated the development of an analytical model of the wing and aircraft structure that accurately predicted modal characteristics. Prediction of flutter speeds at various flight altitudes, and development of the Flutter Suppression System (FSS), required use of the modal data.

This paper describes the early flight test experiences which led to a re-evaluation of the composite wing skin design and its representation in the analytical model. Results from static loads and vibration tests which identified the undesirable properties of the original skin and the significant influence of skin-to-frame attachment method on wing torsional stiffness are presented. The logic leading to the skin redesign is discussed and the results of further ground tests are compared to analytical predictions, which show improvement in both skin properties and modeling techniques. The need for future work in matrix-dominant behavior of composite materials is also discussed.

Presented as Paper 82-0676 at the AIAA/ASME/ASCE Structures, Structural Materials, and Dynamics Conference, New Orleans, La., May 10-12, 1982; submitted May 28, 1982; revision received April 21, 1983. This paper is declared a work of the U.S. Government and therefore is in the public domain.

*Aero-Space Technologist, Multidisciplinary Analysis and Optimization Branch, Loads and Aeroelasticity Division, Member AIAA.

†Engineering Specialist, Kentron International.

Wing Design

The ARW-1 planform arrangement, airfoil shape, and twist distribution (at design cruise condition) are similar to those of the earliest version of the "supercritical wing" developed for flight test evaluation.[2] However, the ARW-1 is scaled in size for use with the Firebee II vehicle. The DAST ARW-1 arrangement is shown in Fig. 1.

The design requirements for ARW-1, with regard to structural strength and stiffness, were: 1) the wing shall withstand maneuver loads from -1.5 to $+2.5$ g with an ultimate factor of safety of 1.25, and 2) the wing shall have bending and torsion characteristics such that unsuppressed flutter occurs within the flight envelope. Other requirements that influenced the design were: 1) that the wing should be fabricated of conventional-type structure, that is, spars, stringers, ribs, and an external skin, and 2) that the wing skins should be nonbuckling in shear and compression at all test conditions in order to avoid any disturbance of the supercritical airfoil shape.

The requirement that the wing flutter boundary be within the flight envelope was quite unusual but necessary, in order that an active control system for flutter suppression could be investigated. The normal requirement is for the wing flutter boundary to be well outside the achievable flight envelope.

The structural concept selected to meet the design requirements was 1) to provide sufficient bending stiffness and strength to allow performance of maneuvers, and 2) to provide the low torsional stiffness required so that flutter would occur at the desired flight conditions. Stainless steel spars were used to provide the required wing bending strength and stiffness. The low torsional stiffness could only be achieved through use of a skin material with a very low shear stiffness. The nonbuckling requirement ruled out using a very thin skin. It was determined that a skin of composite material could be thick enough to prevent buckling and still meet the low shear stiffness requirement if the warp direction of all cloth layers of the laminate were oriented parallel to the wing elastic axis. The remainder of the wing structure, that is, the stringers, ribs, and carry-through structure, are of a conventional aluminum alloy. Figure 2 presents a sketch and a photograph showing the wing construction.

Flight Envelope and Flutter Boundary Locations

The calculated flight envelope for the DAST ARW-1 is shown in Fig. 3. The left- and right-hand boundaries of the flight envelope are for straight and level flight at minimum and maximum engine throttle settings, respectively.

The upper boundary is associated with an angle-of-attack limiter in the flight control system used to avoid a wing pitchup tendency at angles of attack greater than 6 deg. The lower boundary is the minimum altitude that was considered safe to conduct flight tests at the NASA Dryden Flight Research Facility located on the Edwards Air Force Base test range. The flutter boundary location, M_f, that was predicted before flight testing started is also shown in Fig. 3. All launch, routine flight activities, subcritical flutter testing of the wing, and recovery operations are performed in the region to the left of the boundary. All flight in the flutter critical region requires wing stabilization through use of the FSS. The ultimate project goal for the ARW-1 is to demonstrate that the FSS will increase the wing flutter speed by 20%, that is, to $1.2M_f$.

Flight Tests

Three flight tests have been accomplished with the DAST ARW-1.[3-5] During the first flight test, no flutter test data were acquired. During the second flight test, sufficient subcritical testing was accomplished at an altitude of 25,000 ft to establish that the flutter speed was approximately 0.08 Mach number less than the predicted value. Although flight tests of this type are risky, the error in prediction was not of itself a safety problem, since the flight test procedure was established for the purpose of locating the actual flutter boundary. During the third flight test, the wing flutter speed was also established for an altitude of 15,000 ft. Unfortunately, divergent wing oscillations occurred while testing with the FSS on. Severe wing damage resulted, including separation of the right wing panel from the aircraft. The postflight accident investigation determined that FSS-on flutter was encountered because of an incorrect gain value implemented in the FSS.

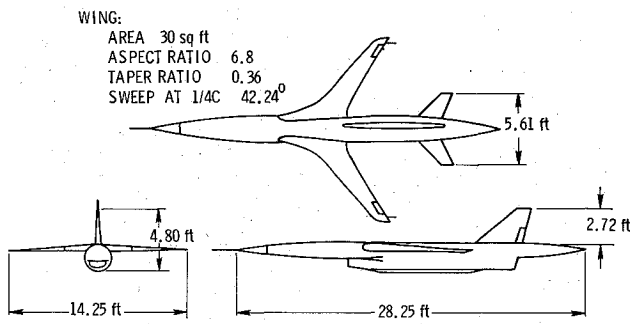

Fig. 1. DAST ARW-1 drone aircraft configuration.

Even though the research wing was extensively damaged, the primary components of the wing structure were salvaged and the wing has been rebuilt. Flight testing resumed in late 1982. A photograph of the DAST ARW-1 taken during the third flight test is presented as Fig. 4.

Postflight Analysis Efforts

Although the difference between the predicted and measured flutter boundary was relatively small ($\Delta M \approx 0.08$), it was larger than desired by the researchers[4] responsible for the development of a FSS capable of providing the 20% increase in flutter speed ($\Delta M \approx 0.16$). Therefore, starting after the second flight test and with increased emphasis after the third flight test, the entire flutter analysis effort was re-evaluated, particularly with regard to the accuracy of the structural model.

From modal analysis, it was known that small changes in wing structural characteristics were noticeable in the form of mode frequency changes, but that little observable change occurred in mode shapes. Therefore, an analysis of flutter speed sensitivity to variations in the two primary wing structural mode frequencies was performed by holding the modal shapes constant and arbitrarily varying the mode frequencies. Whereas flight flutter testing was performed by flying at constant altitude and varying flight speed, it is more convenient to perform flutter analyses by holding speed constant and varying density or altitude. The sensitivity analysis was performed for a Mach number of 0.90. The results, presented in Fig. 5, show that the predicted flutter boundary did not change significantly with changes in the wing first bending mode frequency. However, a very significant variation in the predicted flutter boundary was related to changes in torsion mode frequency, which emphasized the need to accurately predict the frequency of this mode.

Wing Skin Shear Stress-Strain Characteristics

For the ARW-1 flight tests performed, the wing skins were a laminate of seven layers of 181-style fiberglass cloth preimpregnated with a polyester resin (matrix) with the warp direction of all cloth layers oriented parallel to the wing elastic axis. For this layup, the laminate shear modulus is primarily dependent on matrix (resin) properties rather than fiber properties, which is in contradiction with the general practice for composite structure design.[6] Figure 6 presents values of shear stress shear strain as determined from an average of five coupon samples tested at room temperature by the methods of

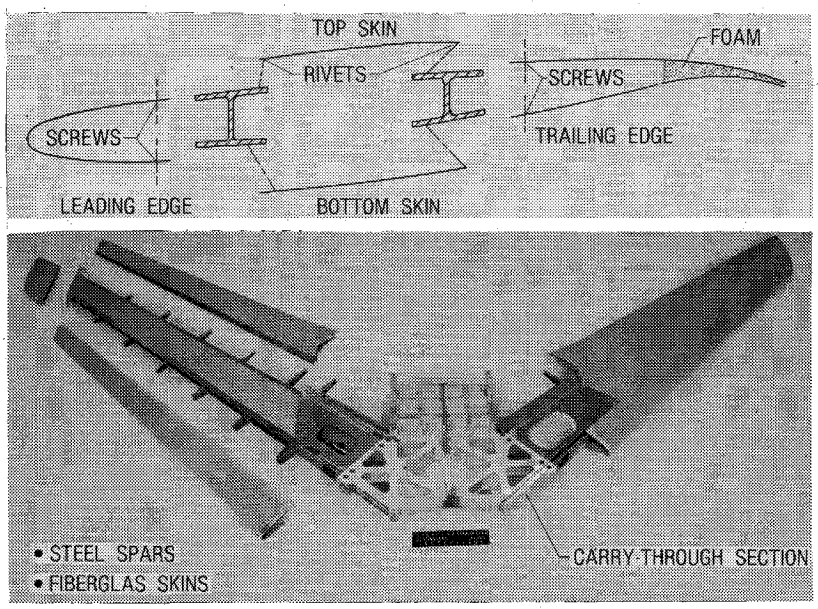

Fig. 2 Research wing construction.

Ref. 7. The nonlinear shear stress-/strain curve is typical of composite materials primarily due to the viscoelastic properties of the matrix.[8-11]

After ARW-1 flight testing was in progress, a 120-style fiberglass fabric preimpregnated with epoxy resin was evaluated for use as the skin for another DAST wing. Shear stress-strain test results for the glass/epoxy material are presented in Fig. 7 for three temperatures. As the test temperature is reduced, the material exhibits increased shear stiffness, more linear response, and substantially less hysteresis. Creep is evident from the failure of the shear strain to return to zero when the shear stress is removed.

Shear Modulus Determination

The shear modulus, G, of a material is defined as the relationship between shear stress, τ, and shear strain, γ, ($G=\tau/\gamma$). Because, as described above, the lamina (laminate layer) shear stress-strain relationships are nonlinear, it is necessary to define the shear modulus property of the glass/polyester and glass/epoxy materials as a function of shear load rather than as a single value. Two methods of defining shear modulus values as a function of shear load are the tangent slope and secant slope methods. The tangent method defines the shear modulus as the slope of the shear stress-strain curve as a function of shear stress level. The secant method defines the modulus as the slope of a line from the origin to a point on the curve corresponding to the shear stress level. As can be seen from the hysteresis loop curves of Fig. 7, both methods would define different shear modulus values for the upload and download curves.

Neither method of defining shear modulus appears to be totally satsifactory for the ARW-1 application because of concern about using a shear modulus value obtained from static tests for a condition where the material is subjected to a combination of static and dynamic loading, that is, analysis of modal characteristics for flight test conditions where the

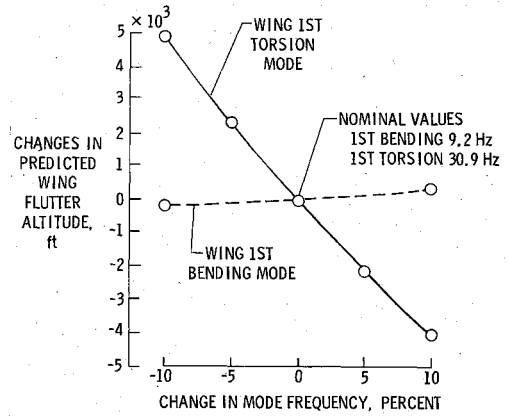

Fig. 5 Flutter sensitivity to changes in structural mode frequencies.

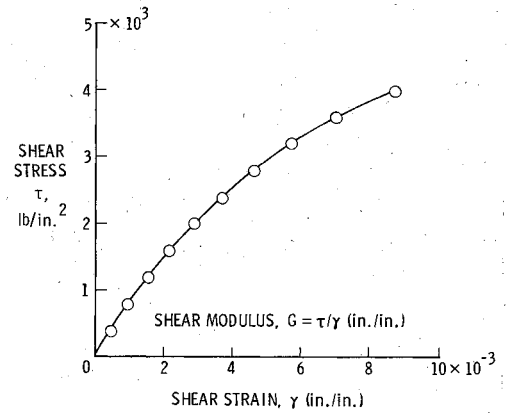

Fig. 6 Shear stress-strain curve for the glass/polyester material at room temperature.

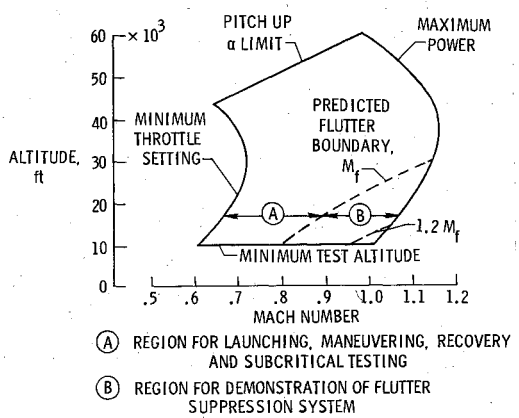

Fig. 3 ARW-1 flight envelope and predicted flutter boundary.

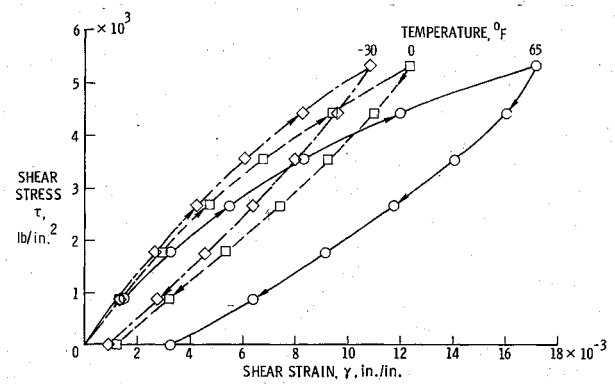

Fig. 7 Shear stress-strain curve for the glass/epoxy material.

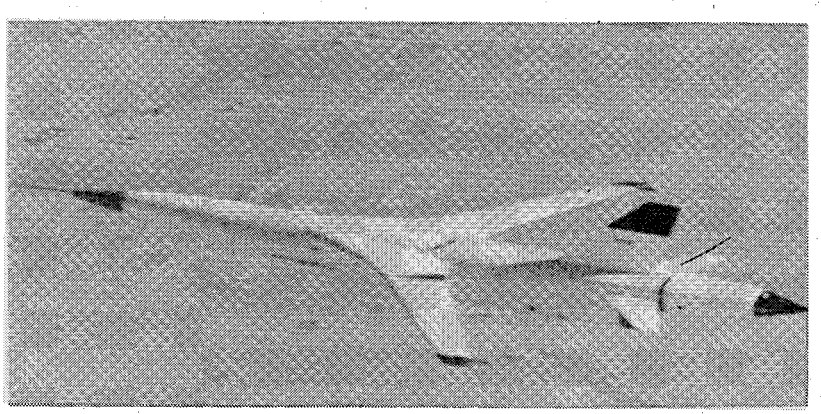

Fig. 4 DAST vehicle with ARW-1.

material is also subjected to large shear loads. However, the secant method was selected since it tends to average the slopes of the upload and download curves. Secant shear modulus values for the upload curve are shown in Fig. 8 for both the glass/polyester material (used on the flight tests performed) and the glass/epoxy material.

Prior to the start of flight testing, the wing skin shear loads had been estimated to range from 100 to 1000 psi. However, strain gage bridge and wing surface pressure measurements taken during flight testing indicated that higher torsion loads were experienced during flight flutter testing than previously considered. Postflight predictions of the maximum wing skin shear stress levels expected for flutter flight test conditions up to the $1.2M_f$ boundary are presented in Fig. 9. As can be seen from the figure, the wing skins between the front and rear spars would be subjected to the largest shear loads (2000-3000 psi). It was concluded that different shear modulus values would be required for each region of wing skin and that the value used should be appropriate for the shear stress levels and temperatures associated with the ground or flight test condition being analyzed in order to accurately predict the torsion mode frequency.

Reference 12 provides another example of how matrix-dominant properties complicated the analysis of a tailored composite wing. These experiences indicate the need for a better understanding of the properties that are primarily influenced by matrix characteristics.

Skin Laminate Modification

During the process of rebuilding the wing, consideration was given to replacing the wing centerbox skins with a laminate that included some layers rotated to a ±45 deg orientation. For shear loading conditions, this would change the laminate from being matrix dominate to one that was partially influenced by fiber characteristics. The change would reduce shear stress-strain nonlinearities and, therefore, also reduce the variation in shear modulus associated with the range of shear stress expected for the various skin panels. The skin thickness would have to be reduced in proportion to the resulting increase in shear modulus in order to maintain the previous level of skin shear stiffness. The glass/epoxy material was more appropriate for this purpose than the original glass/polyester material since: 1) it had a lower shear modulus, 2) the basic lamina exhibited less nonlinearity, and 3) the thickness of each laminate layer was about one-third that for the material used previously (0.0036 vs 0.010 in./layer) which allowed more flexibility in the tailoring of the laminate characteristics.

A composite consisting of 15 layers of glass/epoxy with 4 layers at a 45 deg orientation $[0_5, \pm 45, 0, \pm 45, 0_5]$ was selected for the replacement laminate. The total thickness of the replacement laminate is 0.054 in., as compared with a design thickness of 0.070 in. for the original laminate. A comparison of the shear stiffness of the replacement and original laminates, which includes the effect of differences in skin thickness, is shown in Fig. 10. The new laminate has less initial shear stiffness and a considerable reduction in nonlinear shear response. The reduction is due both to the rotated laminate layers and the change of materials. With the replacement skin laminate used for the higher loaded centerbox skins, the resulting overall variation in wing torsion stiffness expected during flight testing has been substantially reduced. In order to compensate for the reduction in skin thickness and comply with the nonbuckling design requirement, it was necessary to add some local skin stiffening at the root region of the wing.

Validation of Structural Modeling

A series of finite-element models (FEM) of the wing and aircraft structure have been used for both static analysis and the determination of natural modes and frequencies. A

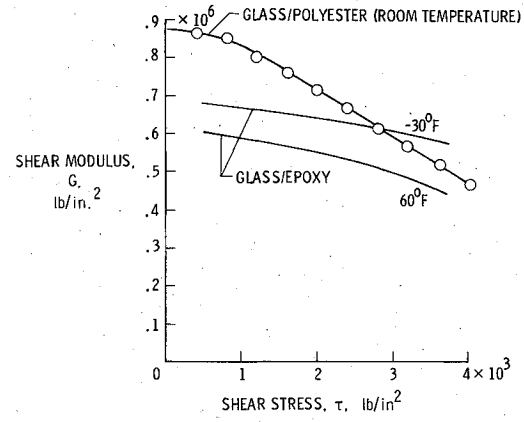

Fig. 8 Composite material shear modulus variation with shear stress.

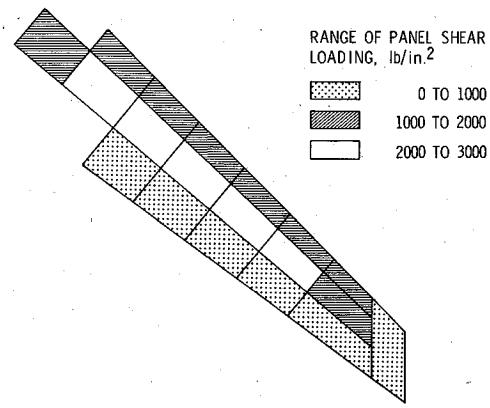

Fig. 9 Shear loads on wing skin panels.

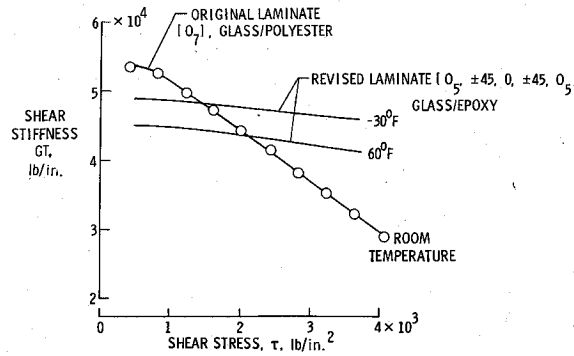

Fig. 10 Laminate shear stiffness variation with shear stress.

NASTRAN[13] FEM (see Fig. 11) was used for the wing design effort and for analysis efforts in support of the flight tests performed. Later an engineering analysis language (EAL)[14] FEM was developed (see Fig. 12). The EAL FEM incorporates a finer nodal mesh, includes the wing glove fairings, and, in some instances, uses more representative structural elements. During the process of rebuilding the DAST ARW-1, careful attention was given to assuring that the finite-element analytical model of the wing structure contained an accurate description of mass and stiffness. To accomplish this, a series of mass, center of mass, static loads, and vibration tests were performed for comparison with predictions from comparable analytical models. For the comparisons discussed in this section, the tests were performed using the wing centerbox structure, which consists of the front and rear spars, ribs, stringers, and upper and lower centerbox skins. The simplified EAL FEM used to provide predictions for these tests is shown in Fig. 13.

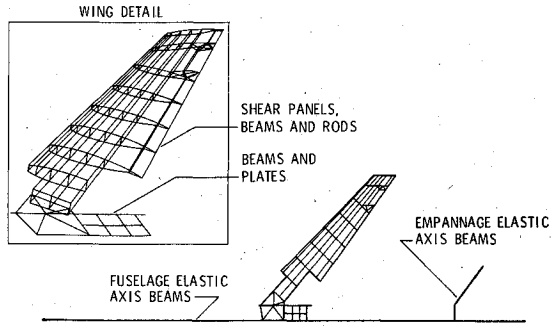

Fig. 11 NASTRAN finite-element model of DAST ARW-1.

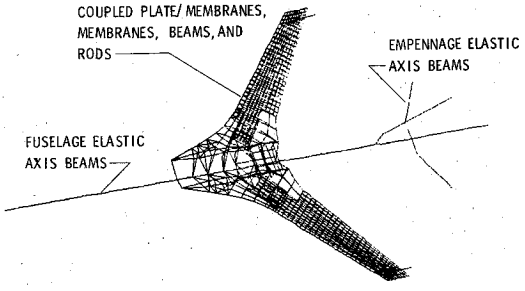

Fig. 12 EAL wing and fuselage model.

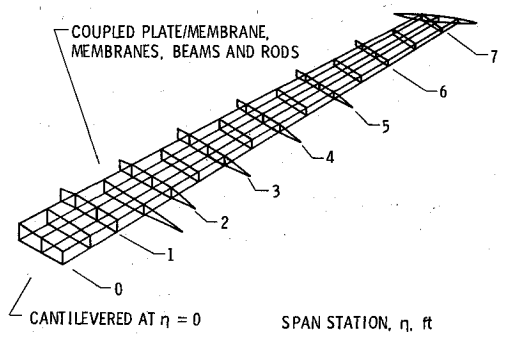

Fig. 13 Simplified EAL model of wing centerbox.

The first wing centerbox structural configuration tested utilized glass/polyester laminate skins similar to those of the original wing. However, in addition to riveting, the skins were now bonded to the wing spars and stringers. Bonding was added because, following the second flight test, evidence of some "working" of rivet heads had been observed. The centerbox structure was cantilevered off a backstop and tested for vertical bending stiffness, torsional stiffness, and natural vibration frequencies. Figure 14 shows that, for a vertical bending load, good correlation was obtained between predicted and measured vertical displacements, whereas the upper two curves of Fig. 15 indicate poor correlation of predicted and measured twist deflection for a torsional load.

Similarly, Table 1 shows good correlation for bending vibration modes, but that the first torsion frequency was much higher than initially predicted. Since both static and vibration tests indicated the actual wing was substantially stiffer in torsion than predicted, the problem was not attributed to skin nonlinear shear stress-strain characteristics as this would tend to reduce stiffness under torsion load. Correction of the discrepancy was required because of the dependence of flutter on wing torsional stiffness. The problem was found to be in the model representation of skin-to-frame attachment. Once this phenomena was properly accounted for, as described below, the revised predictions in Fig. 15 and Table 1 resulted.

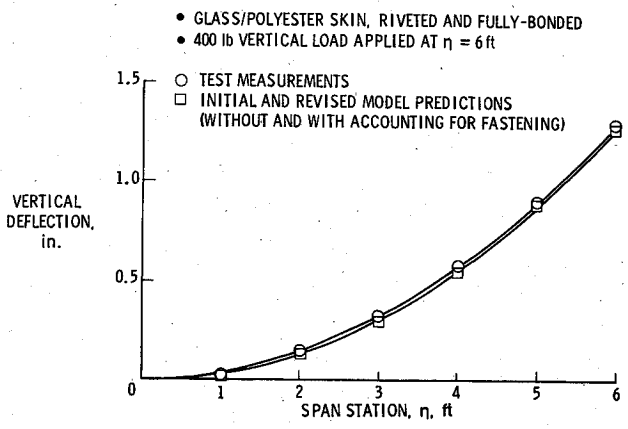

Fig. 14 Wing centerbox bending (glass/polyester skins).

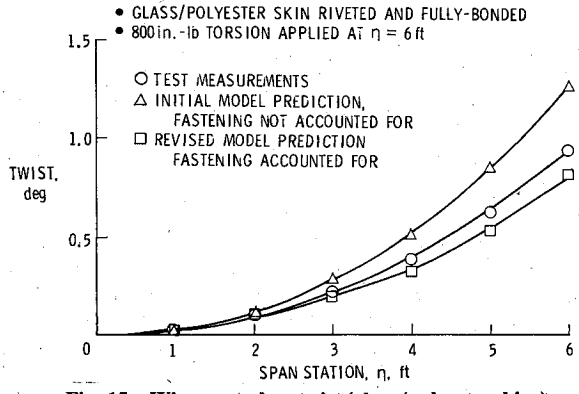

Fig. 15 Wing centerbox twist (glass/polyester skins).

Table 1 Natual frequencies of cantilevered centerbox with fully bonded glass/polyester skin

Mode	Frequency, Hz		
	Test	Initial[a] Prediction	Revised[b] Prediction
First vertical bending	14.4	14.4	14.4
First in-plane bending	50.8	51.5	53.9
Second vertical bending	59.6	60.2	60.5
First torsion	82.5	66.0	81.8

[a] Bonding not accounted for.
[b] Fastening accounted for.

Table 2 Natural frequencies of cantilevered centerbox with partially bonded glass epoxy

Mode	Frequency, Hz	
	Test	Prediction[a]
First vertical bending	14.3	14.2
First in-plane bending	50.8	51.8
Second vertical bending	59.2	59.4
First torsion	72.8	70.0

[a] Fastening accounted for.

The wing skins were defined in the model as being continuous from the front spar vertical web to the rear spar vertical web as shown in Fig. 16. However, the method of fastening the wing skins to the wing frame (i.e., spars, stringers, and, ribs) was not modeled. The shear flow path for the FEM is shown in the upper part of Fig. 17. In reaction to a torsion load, the shear flow path is from the front spar vertical web, to the upper surface skin, to the rear spar vertical web, and back through the lower surface skin. In actuality, due to bonding, a much greater portion of the shear

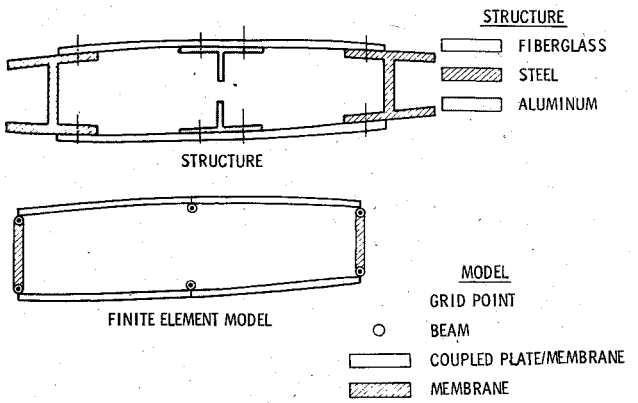

Fig. 16 Comparison of structure and model centerbox cross sections.

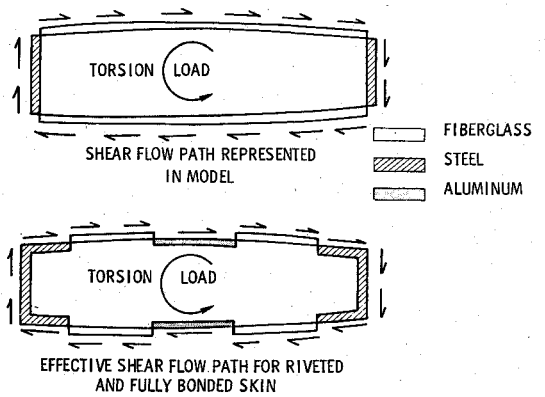

Fig. 17 Comparison of model and effective shear flow paths.

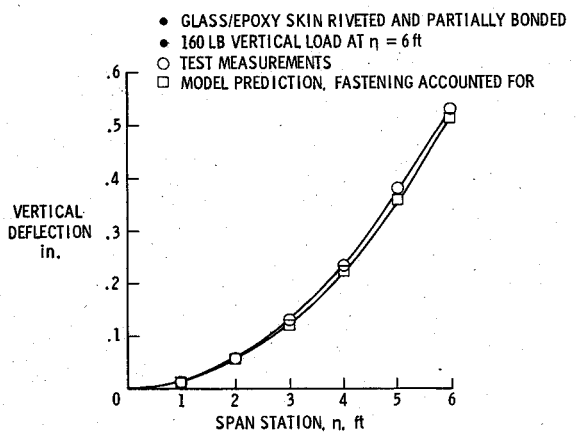

Fig. 18 Wing centerbox bending (glass/epoxy skins).

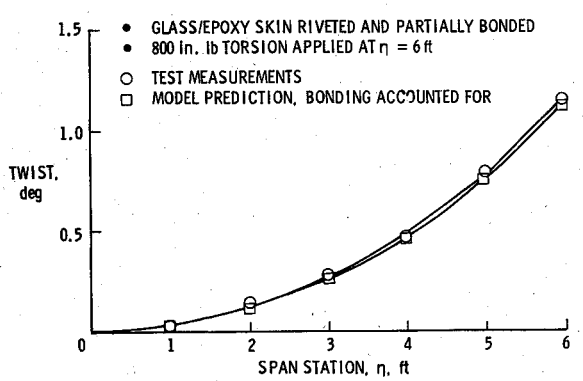

Fig. 19 Wing centerbox twist (glass/epoxy skins).

flow path is through the stiffer metal components, that is, the spar and stringer flanges. In the bonded regions, the skin and the spar flange and stringer base essentially act together. Because the spar flange and stringer are so much stiffer in shear than the fiberglass skin, the effective shear flow path is more like that shown in the lower protion of Fig. 17. If the skins are only fastened by riveting, the stiffening effect in torsion is reduced, but still must be accounted for.

The increased torsional stiffness due to effective shear flow path was approximated by computing an equivalent skin shear modulues, G_e, for each model skin element using Castigliano's Theorem.[15] The following expresion, for example, can be derived for the single cell in the lower portion of Fig. 17.

$$G_e = \frac{S_e}{t_g\left[\frac{S_b}{G_a t_b} + \frac{S_f}{G_s t_f} + \frac{S_g}{G_g t_g}\right]}$$

where

G = shear modulus
S = distance along mean periphery
t = wall thickness

and where the subscripts indicate the following:

a = aluminum
b = stringer base
e = equivalent fiberglass
f = spar flange
g = actual fiberglass
s = steel

The rebuilt wing centerbox structure with glass/polyester skins fully bonded to the spars and stringers was stiffer in torsion than desired. Because of this and concern over the nonlinear shear stress-strain properties discussed earlier, the skins were removed and replaced with the glass/epoxy skin laminate $[0_5, +45, 0, +45, 0_5]$. Bonding for the replacement glass/epoxy skins was only on the spars and then only in the region between the rivet line and the skin edge. Figures 18 and 19 and Table 2 present comparisons between measured and predicted deflections and frequencies for the centerbox structure with the glass/epoxy skins. The improved correlation between predictions and measurements for this configuration are attributed to the more predictable shear modulus value and the proper accounting for skin-fastening effects.

Concluding Remarks

Difficulties were encountered in the use of a composite laminate skin material for an aeroelastic research wing intentionally designed to flutter. Variations in shear stiffness experienced with the original skin complicated the prediction of flutter characteristics. A revised laminate was selected that includes some layers at a ±45 deg orientation to reduce the nonlinear and temperature effects. It was necessary to compensate for increased shear modulus, however, through reduction of skin thickness. It was also found, as a result of correlating laboratory test results with prediction, that the skin fastening arrangement significantly affected wing torsional stiffness and, therefore, had to be accounted for in both the wing design and the structural model.

Structural tailoring incorporating matrix-dominant properties should always be approached with extreme caution due to the difficulty in predicting variances in behavior. To determine acceptability of such tailoring for future applications, any results from further work in predicting and modeling matrix-dominant behavior would be especially useful. Specific applications may be plausible if careful static and dynamic testing can define behaviorial characteristics under realistically varying conditions. Whenever possible, design solutions using fiber-dominant properties should be sought.

References

[1]Murrow, H.N. and Eckstrom, C.V., "Drones for Aerodynamic and Structural Testing (DAST)—A Status Report," *Journal of Aircraft,* Vol. 16, Aug. 1979, pp. 521-526.

[2]Andrews, W.H., "Status of the F-8 Supercritical Wing Program—Supercritical Wing Technology—A Progress Report on Flight Evaluations," NASA SP-301, 1972.

[3]Edwards, J.W., "Flight Test Results of an Active Flutter Suppression System Installed on a Remotely-Piloted Vehicle," NASA TM 83132, 1981.

[4]Newson, J.R. and Pototzky, A.S., "Comparison of Analysis and Flight Test Data for a Drone Aircraft with Active Flutter Suppression," NASA TM 83145, 1981.

[5]Bennett, R.M. an Abel, I., "Application of a Flight Test and Data Analysis Technique to Flutter of a Drone Aircraft," NASA TM 83136, 1981.

[6]Dastin, S.J., "Composite Materials Fabrication," Design, Fabrication and Mechanics of Composite Materials Seminar, San Francisco, Calif., 1980.

[7]Rosen, B.W., "A Simple Procedue for Experimental Determination of the Longitudinal Shear Modulus of Unidirectional Composites," *Journal of Composite Materials,* Vol. 6, Oct. 1972, p. 554.

[8]Yoshida, H., "Viscoelastic Properties of Fiber-Reinforced Plastics," *Resins for Aerospace Symposium,* edited by C.A. May, American Chemical Society, Washington, D.C., 1980.

[9]Hahn, H.T. and Tsai, S.W., "Nonlinear Elastic Behavior of Unidirectional Composite Laminate," *Journal of Composite Materials,* Vol. 7, Jan. 1973, p. 102-118.

[10]Hahn, H.T., "Nonlinear Behavior of Laminated Composites," *Journal of Composite Materials,* Vol. 7, April 1973, p. 257-271.

[11]Amijima, S. and Adachi, T., "Nonlinear Stress-Strain Response for Laminated Composites, " *Journal of Composite Materials,* Vol. 13, July 1979, p. 206-218.

[12]Monaghan, R.C., "Description of the HiMAT Tailored Composite Structure and Laboratory Measured Vehicle Shape Under Load," NASA TM 81254, 1981.

[13]*The NASTRAN Users' Manual,* NASA SP-222(05), 1978.

[14]Whetstone, W.D., "EISI-EAL: Engineering Analysis Language." *Proceedings of the Second Conference on Computing in Civil Engineering,* American Society Civil Engineers, New York, N.Y., 1980, pp. 276-285.

[15]Bruhn, E.F., "Analysis and Design of Flight Vehicle Structure," Tri-State Offset Company, Cincinnati, Ohio, 1965, p. A6.6.

From the AIAA Progress in Astronautics and Aeronautics Series..

AEROACOUSTICS:

JET NOISE; COMBUSTION ANDCORE ENGINE NOISE—v. 43
FAN NOISE AND CONTROL; DUCT ACOUSTICS; ROTOR NOISE—v. 44
STOL NOISE;AIRFRAME AND AIRFOIL NOISE—v. 45
ACOUSTIC WAVE PROPAGATION; AIRCRAFT NOISE PREDICTION; AEROACOUSTIC INSTRUMENTATION—v. 46

Edited by Ira R. Schwartz, NASA Ames Research Center, Henry T. Nagamatsu, General Electric Research and Development Center, and Warren C. Strahle, Georgia Institute of Technology

The demands placed upon today's air transportation systems, in the United States and around the world, have dictated the construction and use of larger and faster aircraft. At the same time, the population density around airports has been steadily increasing, causing a rising protest against the noise levels generated by the high-frequency traffic at the major centers. The modern field of aeroacoustics research is the direct result of public concern about airport noise.

Today there is need for organized information at the research and development level to make it possible for today's scientists and engineers to cope with today's environmental demands. It is to fulfill both these functions that the present set of books on aeroacoustics has been published.

The technical papers in this four-book set are an outgrowth of the Second International Symposium on Aeroacoustics held in 1975 and later updated and revised and organized into the four volumes listed above. Each volume was planned as a unit, so that potential users would be able to find within a single volume the papers pertaining to their special interest.

v.43—648 pp., 6 x 9, illus.	*$19.00 Mem.*	*$40.00 List*
v. 44—670 pp., 6 x 9, illus.	*$19.00 Mem.*	*$40.00 List*
v. 45—480 pp., 6 x 9, illus.	*$18.00 Mem.*	*$33.00 List*
v. 46—342 pp., 6 x 9, illus.	*$16.00 Mem.*	*$28.00 List*

For Aeroacoustics volumes purchased as a four-volume set: $65.00 Mem. $125.00 List

TO ORDER WRITE: Publications Dept., AIAA, 1290 Avenue of the Americas, New York, N.Y. 10019